Arch. Mech., 40, 5–6, pp. 515–527, Warszawa 1988

Optical method of strain measurements Biaxial tension specimen for birefrigent elastomer

F. BREMAND and A. LAGARDE (POITIERS)

THE METHOD uses a coherent light diffracted by an orthogonal grating engraved on the surface of the specimen. This method has the convenience of giving both in large and small deformations, over a small measuring area, the orientations and the values of the principal extensions as well as the rotation of the rigid body. A simulation of a known deformation field enabled us to test the method. With a measuring base (less than a square milimeter), we used it to compare two cross-shaped tension specimens. Only one shape shown introduces a biaxial stress state in a small region around the central point.

W przedstawionej metodzie pomiarowej wykorzystano światło spójne, ugięte przez ortogonalną siatkę wyrytą na powierzchni próbki. Ma ona tę zaletę, że określa orientację i wartości nie tylko wydłużeń głównych, ale także obrót ciała sztywnego w przypadku dużych i małych deformacji przy małym polu pomiarowym. Symulacja znanego pola deformacji umożliwia testowanie tej metody. Za pomocą bazy pomiarowej (mniejszej niż 1 mm²) zastosowano ją do porównania dwóch rozciąganych krzyżowo próbek. Dzięki temu otrzymano dwuosiowy stan naprężenia wokół punktu centralnego.

В представленном измерительном методе использован когерентный свет, дифрагированный ортогональной решеткой нанесенной на поверхности образца. Имеет он то достоинство, что определяет ориентировку и значения не только главных растяжений, но также вращение жесткого тела в случае больших и малых деформаций, при малом измерительном поле. Имитация известного поля деформации дает возможность тестировать этот метод. При помощи измерительной базы (меньшей чем 1 мм²) метод применен для сравнения двух растягиваемых крестным образом образцов. Благодаря этому, получено двухосевое напряженное состояние вокруг центральной точки.

1. Introduction

FOR A LONG TIME researchers have shown interest in the measurements of large deformations on the surface of an object. They use several techniques. Three gauge rosettes enable access to the three parameters of the Mohr circle of deformations with good linearity and good sensitivity up to 20%. However, they present the inconvenience of not being able to resist successive alternating strains and in addition the measurement base is quite large.

The moiré methods are more difficult to use in the case of large displacements and are not capable of measuring strain greater than 30% and angle greater than 30°. The more useful method in the large deformation field is the grid method which consists in engraving a series of orthogonal lines or a group of circles on the surface of the specimen. The use of circles gives directly the orientations and the values of the principal strains, but the dispersion on the results may go up to 15%. The solution we are proposing is based on the use of two gratings of parallel orthogonal lines (10 lines per mm) marked on the surface of the specimen of which the photographic film is being analysed by the diffraction procedure. This method has already been applied in the case of small deformations [1].

We applied it to measure strains in the central part of two crossed-shaped specimens loaded in a biaxial tension test. A comparison between these two shapes is done and we show that only one leads to the existence of a biaxial stress state in the central point.

2. Principle of the method [2–3–4]

We consider the case of plane deformations on the surface of the specimen. Let us suppose an initial square which is defined in a referential O, X, Y by four points: $O(o, o)$; $A(o, p)$; $B(p, p)$; $C(p, o)$ where p is the length of its sides (Fig. 1).

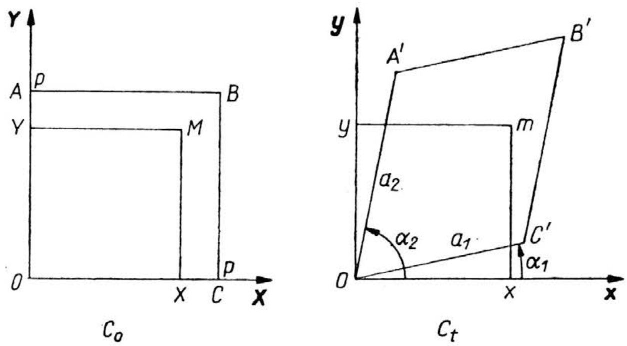

FIG. 1. Deformations of a square.

We suppose this square is transformed into a parallelogram O', A', B', C' in the deformed state such that:

the vector $O'A'$ has components $OA' = (a_2 \cos\alpha_2, a_2 \sin\alpha_2)$,

the vector $O'C'$ has components $OC' = (a_1 \cos\alpha_1, a_1 \sin\alpha_1)$.

Therefore an interior point $M(X, Y)$ is transformed in $m(x, y)$ by the following transformation:

$$x = \frac{a_1}{p} \cos\alpha_1 X + \frac{a_2}{p} \cos\alpha_2 Y,$$

$$y = \frac{a_1}{p} \sin\alpha_1 X + \frac{a_2}{p} \sin\alpha_2 Y.$$

This analytical transformation allows us to determine the gradient of the transformation tensor $\bar{\bar{\mathbf{F}}}$ by the matrix

$$F = \begin{pmatrix} \frac{a_1}{p} \cos\alpha_1 & \frac{a_2}{p} \cos\alpha_2 \\ \frac{a_1}{p} \sin\alpha_1 & \frac{a_2}{p} \sin\alpha_2 \end{pmatrix}.$$

The Cauchy–Green's right tensor $\bar{\bar{\mathbf{C}}} = {}^t\bar{\bar{\mathbf{F}}}\bar{\bar{\mathbf{F}}}$ and Cauchy–Green's left tensor $\bar{\bar{\mathbf{c}}} = \bar{\bar{\mathbf{F}}}{}^t\bar{\bar{\mathbf{F}}}$ have, respectively, the following matrix:

$$C = \begin{pmatrix} \left(\frac{a_1}{p}\right)^2 & \frac{a_1 a_2}{p^2}\cos(\alpha_2-\alpha_1) \\ \frac{a_1 a_2}{p^2}\cos(\alpha_2-\alpha_1) & \left(\frac{a_2}{p}\right)^2 \end{pmatrix},$$

$$c = \begin{bmatrix} \left(\frac{a_1}{p}\cos\alpha_1\right)^2 + \left(\frac{a_2}{p}\cos\alpha_2\right)^2 & \left(\frac{a_1}{p}\right)^2\cos\alpha_1\sin\alpha_1 + \left(\frac{a_2}{p}\right)^2\cos\alpha_2\sin\alpha_2 \\ \left(\frac{a_1}{p}\right)^2\cos\alpha_1\sin\alpha_1 + \left(\frac{a_2}{p}\right)^2\cos\alpha_2\sin\alpha_2 & \left(\frac{a_1}{p}\sin\alpha_1\right)^2 + \left(\frac{a_2}{p}\sin\alpha_2\right)^2 \end{bmatrix}.$$

Now we suppose that the square previously looked for is obtained from an orthogonal grid composed of two gratings of parallel lines of pitch p. These gratings could be either engraved or printed or stick on the surface of a studied specimen. If we assume the grid perfectly follows the displacement in each of the point of the model, we can visualise the deformations of each small initial square.

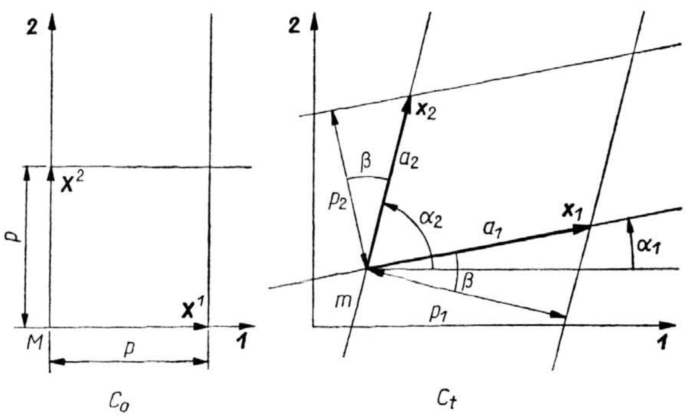

FIG. 2. Deformations of an orthogonal grating.

In accordance with Fig. 2, we write the following relations where β is given by $\beta = \pi/2-(\alpha_2-\alpha_1)$

$$\cos\beta = \frac{p_2}{a_2} = \frac{p_1}{a_1}.$$

Then it is possible to get the components of $\bar{\bar{\mathbf{C}}}$ and $\bar{\bar{\mathbf{c}}}$ in any base by measuring the pitches p_1 and p_2 and the orientations of the two deformed gratings initially orthogonal and of the same pitch p. We will always take the base resulting from the directions of the two initial families of lines.

It is evident that a diagonalisation made on $\bar{\bar{\mathbf{C}}}$ leads to the knowledge of proper values and proper vectors of $\bar{\bar{\mathbf{C}}}$. One can easily obtain the magnitude of the principal strains and the orientation γ' of the proper vectors of $\bar{\bar{\mathbf{C}}}$ in accordance with one axis of the referential. The angle γ' represents the direction of the pure principal strains. In fact, generally it is different from γ which visualises the orientation of the principal directions of the strain tensor, and we know the difference $\gamma-\gamma'$ is the rotation of the rigid solid R:

$$\gamma = \gamma' + R.$$

Using the polar decomposition of $\bar{\bar{\mathbf{F}}}$, we show the relation

$$\operatorname{tg} R = \frac{a_2 \cos\alpha_2 - a_1 \sin\alpha_1}{a_2 \sin\alpha_2 + a_1 \cos\alpha_1}.$$

Thus we get the orientation and the value of the principal extensions and the rotation of rigid solid from the knowledge of four parameters (two pitches p_1 and p_2 and two angles α_1 and α_2). These values are obtained using the procedure of diffraction on photographic negatives representing the deformed state of the studied gratings.

The diffraction phenomena of a parallel beam of a coherent light through a plane grating is well known [5, 6]. The hypothesis made in the case of a phenomenon of Fraunhofer's diffraction (infinite diffraction giving regularly spaced points) allow the determination of the pitch of the grating knowing the wavelength λ of the radiation, the distance L between the screen (E) and the photographic film, the distance d between two consecutive points of diffraction

$$p = \frac{\lambda L}{d}.$$

This relation assumes small angles of diffraction, in other words a large value of L with respect to d. When this hypothesis is not verified, we use the relation

$$p = \frac{m\lambda}{\operatorname{Arctg}\dfrac{d^m}{L}},$$

where m is the diffraction order.

We have represented in Fig. 3 the diffraction image of a grating of parallel crossing lines. We notice that the directions formed by the diffraction points are perpendicular

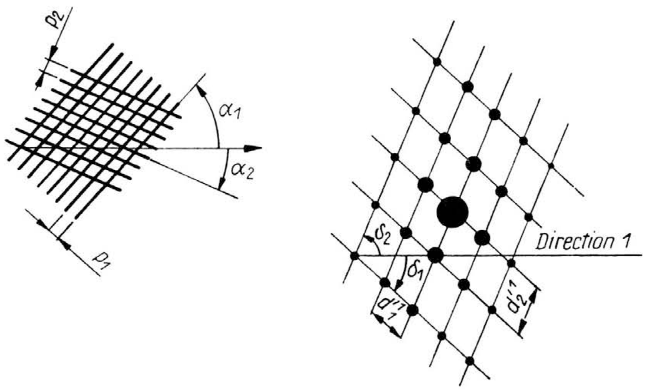

Fig. 3. Diffraction image of a grating.

to the orientation of the family of corresponding lines. It is now easy to describe p_1; p_2; α_1; α_2 as functions of d_1^m; d_2^m; δ_1; δ_2:

$$p_1 = \frac{\lambda m}{\operatorname{Arc\,tg}\dfrac{d_1^m}{L}}, \qquad p_2 = \frac{\lambda m}{\operatorname{Arc\,tg}\dfrac{d_2^m}{L}},$$

$$\alpha_1 = \delta_1 + \frac{\pi}{2}, \qquad \alpha_2 = \delta_2 - \frac{\pi}{2}.$$

The polar coordinates of these points are numerically read by using a digital table. In order to minimise the uncertainties over the four parameters, the center of each point is taken three times. A numerical analysis is done on a microcomputer and it gives the statistical analysis of the data and computes the strain values.

3. **Simulation** [2–3–4]

In order to test the validity of this measuring method, we have made a simulation of an homogeneous strain field. Then, in the deformed state, we consider a grating of pitch p, which is composed of two families of parallel lines but having one inclined with respect to another at an angle $\pi/2-\delta$ (Fig. 4). We suppose these two families are initially

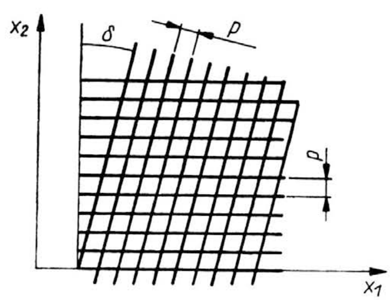

FIG. 4. Geometry of the studied grating.

perpendicular. The transformation from the initial state $(X_1; X_2)$ to the final state $(x_1; x_2)$ has the following expression:

$$x_1 = \frac{1}{\cos\delta} X_1 + \operatorname{tg}\delta X_2,$$

$$x_2 = X_2.$$

We deduce the expression of the gradient of transformation tensor:

$$F = \begin{bmatrix} \dfrac{1}{\cos\delta} & \operatorname{tg}\delta \\ 0 & 1 \end{bmatrix}$$

and the tensors $\bar{\bar{\mathbf{C}}}$ and $\bar{\bar{\mathbf{c}}}$ have the form

$$C = \frac{1}{\cos^2\delta}\begin{bmatrix}1+\sin\delta & 0\\ 0 & 1-\sin\delta\end{bmatrix}, \quad c = \begin{bmatrix}1+\sin\delta & 0\\ 0 & 1-\sin\delta\end{bmatrix}.$$

Since $\bar{\bar{\mathbf{E}}} = \frac{1}{2}(\bar{\bar{\mathbf{C}}}-\bar{\bar{\mathbf{I}}})$ and $\bar{\bar{\mathbf{e}}} = \frac{1}{2}(\bar{\bar{\mathbf{I}}}-\bar{\bar{\mathbf{c}}})$ where $\bar{\bar{\mathbf{E}}}$ and $\bar{\bar{\mathbf{e}}}$ are the Green–Lagrange's tensor and Euler Almansi's tensor, respectively, one can easily write

$$E_1 = \frac{1}{2}\sin\delta\left(\frac{1+\sin\delta}{\cos^2\delta}\right), \quad e_1 = -\frac{1}{2}\sin\delta,$$

$$E_2 = -\frac{1}{2}\sin\delta\left(\frac{1-\sin\delta}{\cos^2\delta}\right), \quad e_2 = \frac{1}{2}\sin\delta.$$

Considering the physical representation of the transformation, we know that the principal directions in the spatial representation are diagonals of the rhomboids.

Hence

$$\gamma = \frac{\delta}{2} + \pi/4.$$

The diagonalisation of $\bar{\bar{\mathbf{C}}}$ leads us to the value of

$$\gamma' = \pi/4.$$

From there we deduce

$$R = \delta/2.$$

We note that the rotation is equal to the variation of the orientation of a diagonal.

The used gratings are identical ($p = 0.042$ mm). Four tests were done with values of δ equal to $-36.5°$; $-27.5°$; $27.5°$ and $36.5°$, the distance L being equal to 1095 mm while the wavelength of the laser beam being equal to 632.8×10^{-6} mm. The experimental

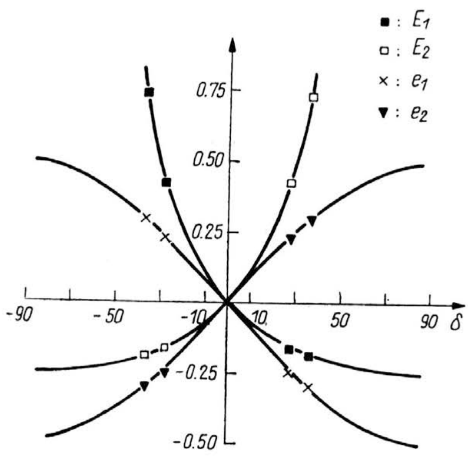

FIG. 5. Principal Lagrangian strains E_1, E_2. Principal eulerian strains e_1, e_2.

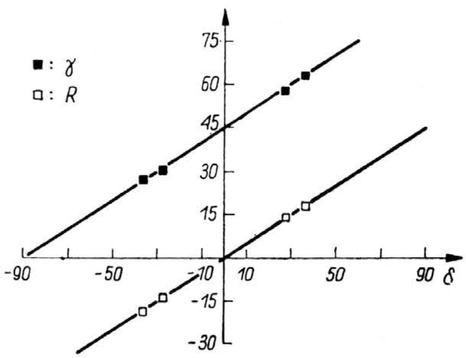

FIG. 6. Orientation of the principal strain and rigid body rotation.

results (Figs. 5 and 6) compare very well with the theoretical curves. It is worth noting that the gratings were of excellent quality and the diffraction points were circular with good contrast.

4. Biaxial tension test [4]

Several biaxial tension specimens have already been used [7, 8, 9]. Their disadvantage is a complex shape: the arms are slotted and the central part is made thinner with fillets at the base of the arms. We have preferred to give priority at the facility of molding taking advantage of the possibilities of our measurement method, and sacrificing somewhat the size of the zone presenting a biaxial state [10].

We used two cross-shaped specimens (Fig. 7) made from a TM60A urethane. In order to limit the influence between the two loading directions, the arms of one shape are made

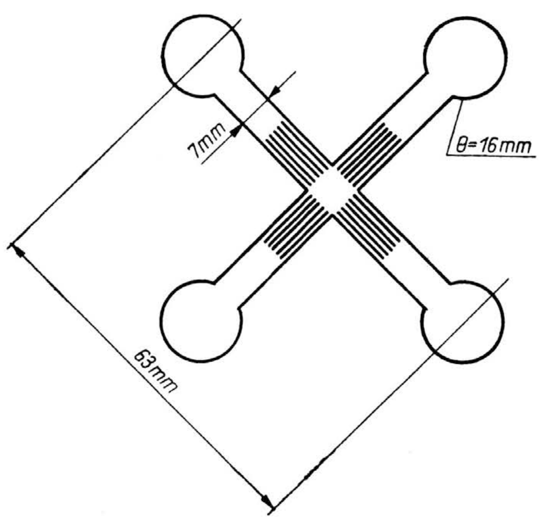

FIG. 7. Geometry of the tension specimen *B*.

of thin strips from the molding [7–8]. In addition, 10 lines of orthogonal gratings (pitch $p = 0.1$ mm) were engraved at the base of the mould and are reproduced on the molded specimens. The tension apparatus has been designed to enable independent loadings in two directions. The forces are transmitted by means of a nylon thread passing over pulleys mounted on rolling bearings.

At first we studied strains all over the central part of each shape. Let us call: specimen A — the classical cross-shaped specimen and specimen B — the shape made with lamellaes. Figure 8 shows the comparison of these two tests where the loading was $F_1 = 4$ kg and

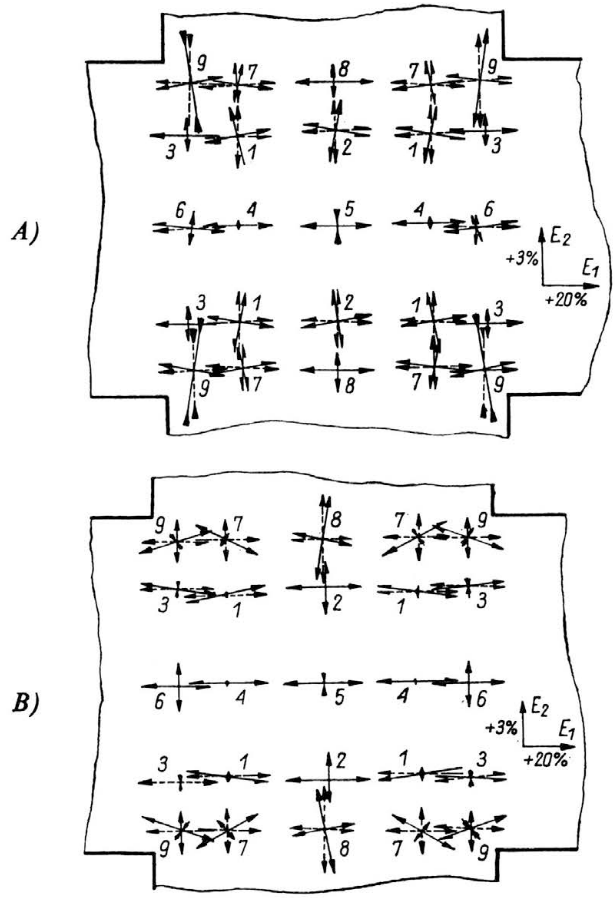

FIG. 8. Comparison between the two specimens. Strains using specimen A. Strains using specimen B.

$F_2 = 2$ kg. In fact, we measured strains in nine points and we used symmetry conditions to extend the values anywhere. The black lines represent the principal deformations. One can note E_2 is smaller than E_1 ($E_2 \simeq \pm 2\%$, $E_1 \simeq 20\%$). We also note a biaxial tension state exists in a little region around the central point 5. Furthermore, the principal and loading directions correspond better for the specimen B than for A in the corner 3, 1, 7, 9.

In a second time we measured the strains ($\varepsilon_1, \varepsilon_2$) and we calculated the stresses (σ_1, σ_2) in the central point 5 of the following procedure:

We suppose the incompressibility relationship to be true

$$\varepsilon_1 \varepsilon_2 \varepsilon_3 = 1,$$

the stresses σ_1 and σ_2 are obtained from the applied forces F_1, F_2 divided by the fictitious section $S_1'(S_2')$ of the arm transmitting the forces (Fig. 9). Knowing the sections $S_1(S_2)$ of these arms in the undeformed state, we have

$$S_1 = l_2 l_3 \quad \text{and} \quad S_1' = \varepsilon_2 l_2 \varepsilon_3 l_3 = S_1/\varepsilon_1$$

and, as a result,

$$\sigma_1 = \frac{F_1 \varepsilon_1}{S_1}, \quad \sigma_2 = \frac{F_2 \varepsilon_2}{S_2}.$$

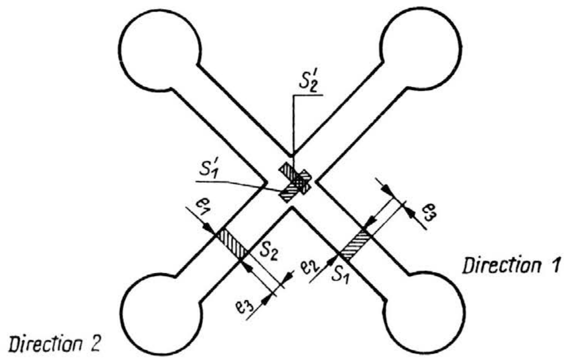

FIG. 9. Determination of the stresses.

These experimental data were compared with theoretical values obtained from a given mechanical behaviour law. Then we supposed the material was incompressible, hyperelastic of neo-Hookean type, and one can easily obtain the following relationship between stress and strain tensor:

$$\bar{\bar{\mathbf{T}}} = p\bar{\bar{\mathbf{1}}} + G\bar{\bar{\mathbf{c}}},$$

where $\bar{\bar{\mathbf{T}}}$ is the Cauchy stress tensor, p represents a hydrostatic pressure function of a point, G is the modulus of rigidity in shear.

Using the incompressibility equation ($c_1 c_2 c_3 = 1$), one can write

$$(\sigma_1 - \sigma_2) = G(c_1 - c_2), \tag{4.1}$$

$$\sigma_1 = G\left(c_1 - \frac{1}{c_1 c_2}\right), \tag{4.2}$$

$$\sigma_2 = G\left(c_2 - \frac{1}{c_1 c_2}\right). \tag{4.3}$$

The first relationship shows the linearity between the difference of the principal stresses and strains (Fig. 10). But the values of G are different and depend on the type of the test

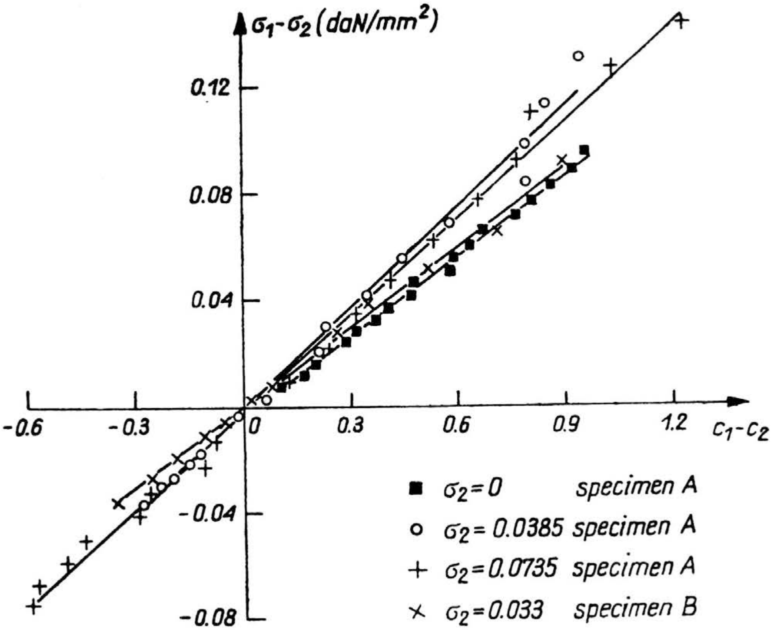

FIG. 10. Linearity between stresses and strain.

and the shape of the specimen. Nevertheless we observe G is the same in the biaxial tension with specimen B and uniaxial tension with specimen A. From Eqs. (4.2) and (4.3) and from this last value of G we computed c_1 and c_2 in function of σ_1 for a given σ_2 (Fig. 11). Then

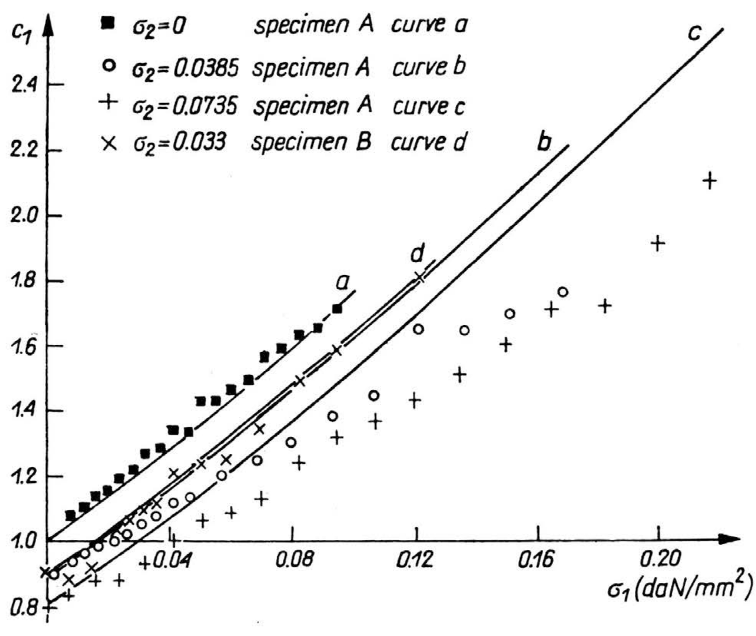

FIG. 11. Strain c_1 versus σ_1 (σ_2 given) in the central point.

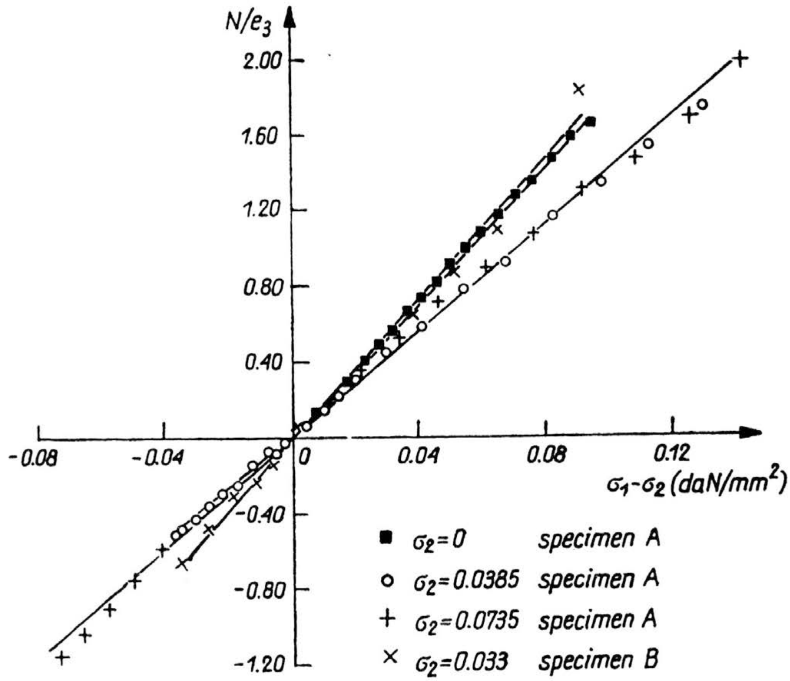

FIG. 12. Fringe order — principal stresses.

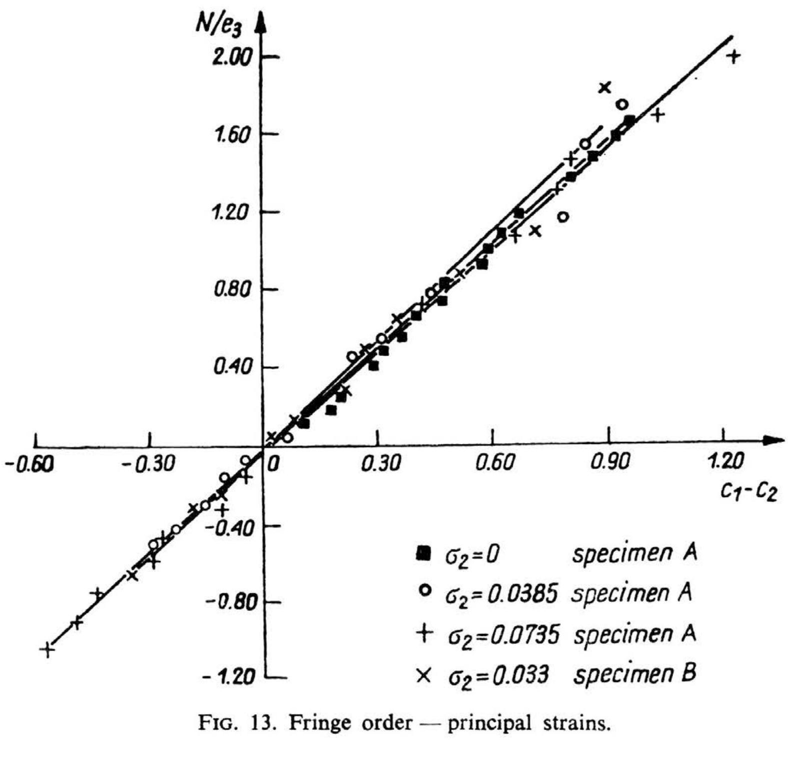

FIG. 13. Fringe order — principal strains.

we note the perfect correspondence between experimental points and theoretical curves *a* and *d*. Hence we deduce that the biaxial tension test done on specimen *B* generalizes the uniaxial test done on specimen *A* but not the biaxial test with *A*. To confirm this, we made birefringence measurements in the central point 5. Then we suppose Maxwell's laws are satisfied even in the finite deformation field. So we can write the linear relationship between N (the fringe order) and $\sigma_1-\sigma_2$ such that

$$N = \frac{Ce}{\lambda}(\sigma_1-\sigma_2), \tag{4.4}$$

where C is the photoelastic constant, e is the thickness of the specimen, λ is the wavelength of the laser beam.

From Eq. (4.4) we obtained Fig. 12 which always shows a comparison between experimental and theoretical data. Again we can see a difference in the proportionality coefficient showing that specimen *A* is not adapted in biaxial tests. Yet if we plot (Fig. 13) the fringe orders versus the principal strains, there is superposition of every curve. It is easy to understand. Alone this last figure is without stresses. We conclude: the problem is in the determination of the stresses which are not very well biaxial using the shape *A* because the loading directions are not independent.

5. Conclusion

Our measuring method leads to the knowledge of orientation and magnitude of the principal strains and of the rigid solid rotation of a small region. It allows to measure strains in the central part of two cross-shaped tension specimens using a 10 lines/mm orthogonal grating. The different results show that only the shape done with lamellae give a biaxial stress state when loading in the biaxial tension test occurs.

References

1. P. J. SEVENHUIJSEN, *The development of a laser grating method for the measurement on strain distribution in plane opaque surfaces*, Presented at the 6th International Conference on Experimental Stress Analysis, 1978 München, VDI — Berichte Nr. 313, pp. 143–147, 1978.
2. F. BRÉMAND, A. LAGARDE, *Méthode optique de mesure des déformations utilisant le phénomène de diffraction*. C.R. Acad. Sci. Paris, 303, Série II, pp. 515–520, 1986.
3. F. BRÉMAND, A. LAGARDE, *Optical method of strain meeasurement. Application to study of circular bending of beam in the large strain range*, Proc. VIIIth International Conference on Experimental Stress Analysis, ed. H. WIERINGA, pp. 341–350, Delft, May 12–16, 1986.
4. F. BRÉMAND, A. LAGARDE, *A new method of optical strain measurement with applications*, SEM Spring Conference Proceedings New-Orleans, pp. 686–694, June 8–13, 1986.
5. J. BRUHAT, *Cours de physique générale — Optique*, 6ème édition revue et complétée par A. KASTLER, Masson et Cie 1965.
6. M. FRANÇON, A. MARÉCHAL, *Diffraction — Structures des images*, Masson et Cie, 1970.
7. E. MÖNCH, D. GALSTER, *A method for producing a defined uniform biaxial tensile stress field*, Brit. J. Appl. Phys., **14**, pp. 810–812, 1963.

8. D. R. HAYHURST, *Experimental testing techniques for high temperature*, Proc. Seventh International Conference on Experimental Stress Analysis, Haifa, Israel, pp. 21–30, 23–27 August 1982.
9. C. ALBERTINI, M. MONTAGNANI, *Dynamic uniaxial and biaxial stress-strain relationship for austenitic stainless steel*, Nuclear Engineering and Design, **57**, pp. 101–123, 1980.
10. F. BRÉMAND, A. LAGARDE, *Sur une forme simple d'éprouvettes de traction biaxiale pour un élastomère. Application à la détermination de lois de comportement mécanique et optico-mécanique en grandes déformations*, C.R. Acad. Sci. Paris, 305, série II, pp. 929–934, 1987.

LABORATOIRE DE MECANIQUE DES SOLIDES
EQUIPE DE RECHERCHE ASSOCIEE AU C.N.R.S., POITIERS, FRANCE.

Received March 24, 1988.